**FULL PAPER**

Topographical Micropatterns

ADVANCED
OPTICAL
MATERIALS

www.advopticalmat.d

# Assembly of Topographical Micropatterns with Optoelectronic Tweezers

*Shuailong Zhang, Yifan Zhai, Ran Peng, Moein Shayegannia, Andrew G. Flood, Juntian Qu, Xinyu Liu, Nazir P. Kherani, and Aaron R. Wheeler\**

Topographical micropatterns (TMPs), or ordered arrays of 3D features on a flat surface, have become important for a wide range of applications. A new optofluidic method based on optoelectronic tweezers to assemble TMPs from suspensions of microparticles in fluid is reported. After assembly, TMPs can be freeze-dried and then transferred to alternate substrates. 3D simulations are carried out to clarify the experimental results and techniques are developed to evaluate pattern-transfer fidelity, which is found to be >90% for a wide range of different structures. The optofluidic assembly method described here is facile and accessible, suggesting utility for a wide range of microfabrication and microassembly applications in the future.

## 1. Introduction

Topographical micropatterns (TMPs), which comprise ordered arrays of 3D features on a flat surface, have emerged as an important tool for myriad applications, ranging from photonic identifiers and sensors[1–4] to cell/particle sorting and sequestration.[5–7] There are three categories of techniques that have been used to manufacture TMPs; the first (canonical) category relies on photo- or electron-beam (e-beam) lithography and etching. These methods permit unparalleled flexibility in user determination of feature size and spatial positioning, but they are expensive, require a cleanroom (and are not accessible to all users), and have some limitations on throughput (particularly for e-beam lithography). In recognition of these limitations, a second category of "dry" cleanroom-free methods has been developed, including 3D printing,[8–10] laser machining,[11] and "pick-and-place" technologies.[12,13] These techniques are useful, but they also rely on expensive and specialized tools and well-trained personnel, and can have limited throughput.

A third category of "wet" cleanroom-free techniques has recently been proposed for forming topographical micropatterns, relying on dielectrophoresis tweezers (DEPT),[14–16] acoustic tweezers (AT),[17–19] magnetic tweezers (MT),[20,21] and optical tweezers (OT).[22–25] These techniques, in which patterns of 3D particles are assembled in a fluidic environment and are later dried for use in TMP applications, are creative and interesting, and preserve many of the advantages of the canonical methods while allowing for accessible, cleanroom-free operation. But each of the individual techniques has disadvantages; for example, DEPT and AT require the manufacture of micropatterned electrodes (typically using canonical cleanroom methods) and lack the flexibility to pattern large numbers of features. Likewise, MT-based methods can only assemble micro-objects that respond to magnetic fields, and OT-based techniques have sub-nanoNewton (<nN) manipulation forces, which sets firm limits on the type and size of micro-objects that can be assembled. Additionally, while it is possible to control multiple micro-objects in parallel with OT, these systems require complex beam shaping optics with specialized control software. These challenges and others are substantial and are at least part of the reason that the third category of TMP assembly techniques is (currently) relegated to proof-of-concept work in research labs.

Here, we report a new technique for design and manufacture of TMPs, relying on optoelectronic tweezers (OET).[26–41] The new method is a member of the wet cleanroom-free assembly techniques, but lacks many of the limitations indicated previously. In this report, we describe the use of the new technique to form TMPs from suspensions of polystyrene microbeads, metallic

Dr. S. Zhang, Prof. A. R. Wheeler
Donnelly Centre for Cellular and Biomolecular Research
University of Toronto
Toronto, ON M5S 3E1, Canada
E-mail: aaron.wheeler@utoronto.ca

Dr. S. Zhang, Prof. A. R. Wheeler
Department of Chemistry
University of Toronto
Toronto, ON M5S 3H6, Canada

Dr. S. Zhang, Y. Zhai, Prof. A. R. Wheeler
Institute for Biomaterials and Biomedical Engineering
University of Toronto
Toronto, ON M5S 3G9, Canada

Dr. R. Peng, J. Qu, Prof. X. Liu
Department of Mechanical and Industrial Engineering
University of Toronto
Toronto, ON M5S 3G8, Canada

M. Shayegannia, A. G. Flood, Prof. N. P. Kherani
Department of Electrical and Computer Engineering
University of Toronto
Toronto, ON M5S 3G4, Canada

Prof. N. P. Kherani
Department of Materials Science and Engineering
University of Toronto
Toronto, ON M5S 3E4, Canada

The ORCID identification number(s) for the author(s) of this article can be found under https://doi.org/10.1002/adom.201900669.
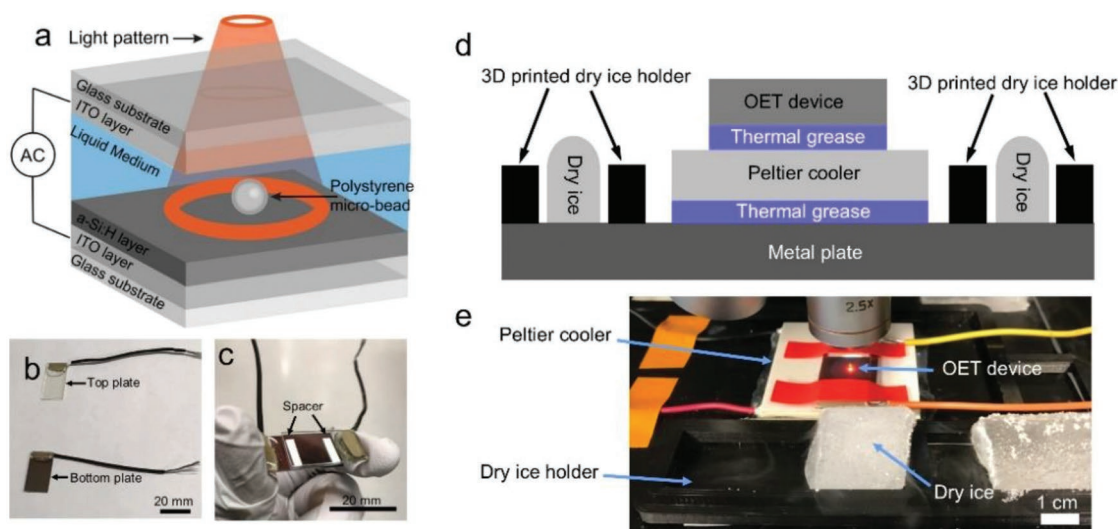
**Figure 1.** An optoelectronic tweezers (OET) based method for forming topographical micropatterns (TMPs). a) 3D schematic of an OET device with top and bottom plates. The bottom plate features a layer of photoconductive material (dark gray), in this case hydrogenated amorphous silicon (a-Si:H). A light pattern (orange) is projected onto the photoconductive layer through a microscope. b) Picture of a top and bottom plate of an OET device. c) Picture of an assembled OET device. d) Cross-sectional schematic of the cooling stage used to form transferrable TMPs. e) Picture of the cooling stage assembled with an OET device on a microscope.

microspheres, and graphene nanoplatelets, which are then freeze-dried and transferred onto a variety of flexible and rigid substrates for characterization. We propose that the new method presented here is versatile and powerful, and may eventually be useful for a wide range of applications for TMPs in the future.
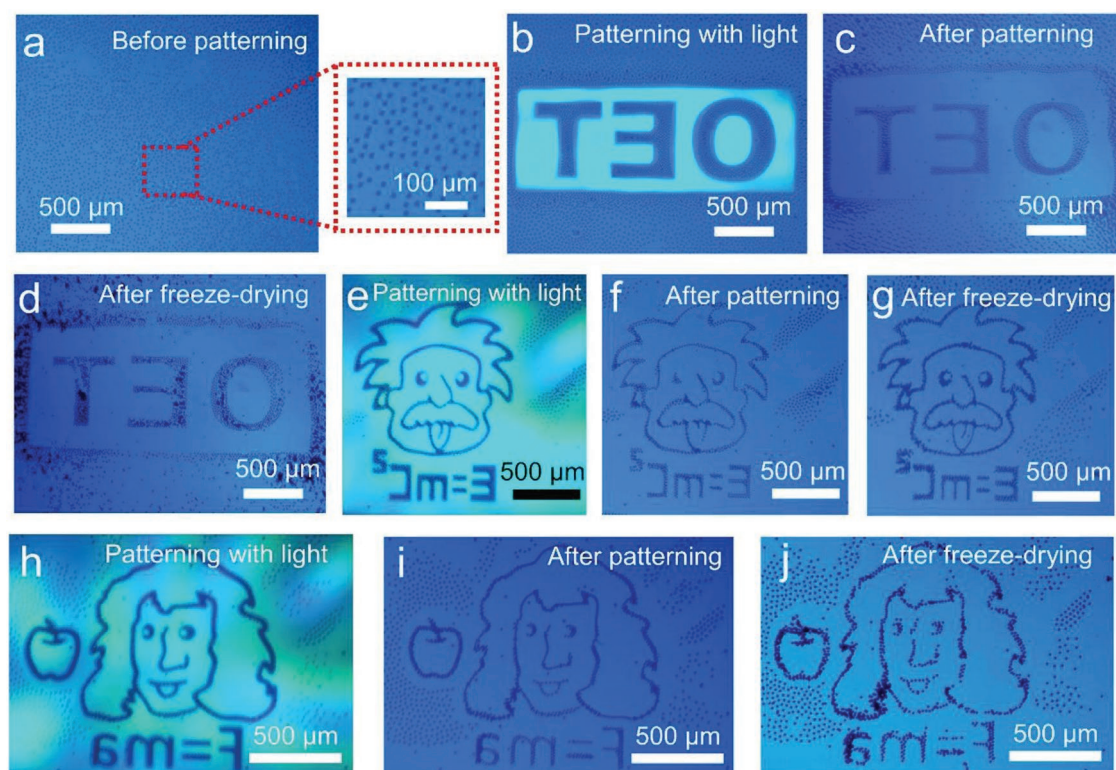
## 2. Results and Discussion

The methods introduced here rely on OET, an accessible technique that requires only a microscope, a consumer-grade projector, and an inexpensive device coated with a photoconductor. **Figure 1**a is a schematic of the OET devices used in this work, which comprise a top and a bottom plate, each coated on one side with conductive, transparent indium tin oxide (ITO). The ITO on the bottom plate was coated with hydrogenated amorphous silicon (a-Si:H) (Figure 1b).[35,40,41] OET devices were assembled by joining the top and bottom plates together with a spacer to form a chamber (Figure 1c), within which the manipulation of microparticles was performed. The OET phenomenon relies on the unique characteristics of the photoconductive layer (in this case, a-Si:H). In the dark, the impedance of the a-Si:H is very high and the applied AC potential mainly drops across this layer. However, when the device is illuminated by light, the impedance of the a-Si:H is reduced significantly, such that the voltage drops predominantly across the liquid medium above the illuminated area. The resulting nonuniform electric field interacts with the samples in the liquid medium producing either repulsive (negative DEP) or attractive (positive DEP) force depending on the signs of the Clausius–Mossotti (CM) factors of the system.[16] The CM factor can be tuned by changing the complex permittivity of the particle or the suspending medium, or by changing the frequency of the applied field.

Here, we combine (i) the assembly of TMPs in liquid by OET, with two new functions: (ii) freeze-drying of the TMPs and (iii)

transfer to alternate substrates. Functions (i) and (ii) were enabled using a custom microscope stage insert bearing dry ice and a Peltier cooler (Figure 1d,e), and **Figure 2** outlines the process. As shown in Figure 2a, TMP formation begins with a random suspension of particles in liquid—in this case, 10 µm diameter polystyrene microbeads. As shown in Figure 2b (extracted from Movie S1, Supporting Information), a light pattern is projected onto the suspension of particles—in this case, a mirror image of the abbreviation, "OET." Figure 2c shows a microscope image of a TMP after assembly (in liquid medium). The CM factor for polystyrene microbeads in the conditions used here results in negative DEP force, such that the particles are repelled from the illuminated region and accumulate in the dark region.[40] Thus, when handling polystyrene particles, the light patterns were projected as a "negative" of the intended TMP. Finally, Figure 2d shows an assembled TMP after freeze-drying. In this step, the aqueous medium is flash-frozen, after which it sublimates directly to the vapor phase. As shown, the TMP is well preserved during this process, suggesting that potentially disruptive fluidic forces caused by freezing and sublimation are small relative to the negative DEP forces that keep the particles in position. (In preliminary work with room-temperature evaporation, the fluidic forces were found to be substantially more disruptive.)

The freeze-drying method reported here was inspired by a previous report[41] of freeze-drying a pattern of objects formed by OET. In the previous report,[41] particles were painstakingly assembled one-by-one (up to a total of 12 particles) prior to freeze-drying. This original technique is interesting, but quite slow, and the small number of particles limits the complexity of the resulting patterns. In the new method reported here, the TMPs feature thousands (or more) particles that are simultaneously assembled, in a process that requires less than a minute of OET image projection. This method is quite versatile, limited only by the user's imagination—for example, it is

1900669 (2 of 7)

**ADVANCED
SCIENCE NEWS**
www.advancedsciencenews.com

**ADVANCED
OPTICAL
MATERIALS**
www.advopticalmat.de

**Figure 2.** Formation and freeze-drying of TMPs from 10 μm diameter polystyrene microbeads using OET. a) Bright-field microscope image of an unpatterned suspension of beads on an OET device. The inset (red dashed box) features a magnified view of the beads. b) Bright-field microscope image showing the illumination of the microbead suspension with a negative, mirror-image light pattern spelling "OET." c,d) Bright-field microscope images of the assembled "OET" TMP in suspension and after freeze-drying. e,h) Bright-field microscope images showing the illumination of the microbead suspension with a light pattern depicting a negative, mirror image of a stylized caricature of Albert Einstein with the mass energy equation and Isaac Newton with an apple and the second law of motion. Bright-field microscope images of the assembled Einstein and Newton TMPs f,i) in suspension and g,j) after freeze-drying. Some of the images in this figure were extracted from Movie S1 (Supporting Information).

straightforward to form TMPs featuring stylized caricatures of Albert Einstein (Figure 2e–g) and Isaac Newton (Figure 2h–j). We have formed hundreds of similar structures without incident, and propose that this is a robust new technique for forming topographical micropatterns.

The method described above is useful for (i) forming wet TMPs using OET, and (ii) removing the liquid to dry the

TMPs. We were curious about the timing of the process in (i) and decided to characterize the pattern formation. Numerical simulations were carried out to provide insights into the assembly process (see Figure S1, Supporting Information), and experiments were conceived to allow the monitoring of pattern formation in real time. **Figure 3**a–f shows bright-field microscope images of a wet microbead-based TMP at 0, 0.8,
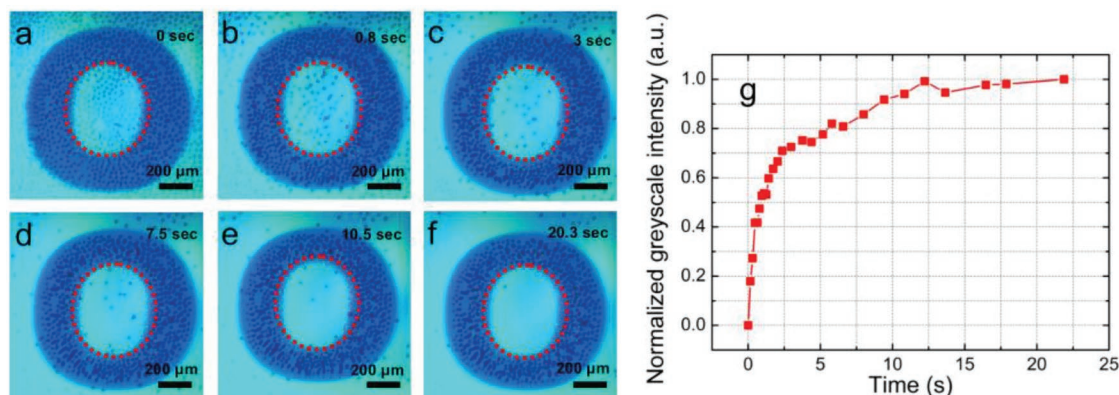


**Figure 3.** Dynamics of TMP assembly. a–f) Bright-field microscope images collected during the assembly of a TMP from 10 μm diameter polystyrene microbeads at 0, 0.8, 3, 7.5, 10.5, and 20.3 s after projecting the light pattern. The number of microbeads inside the dashed red circle decreases as time passes. g) Plot of normalized greyscale intensity of the area inside the red dashed circle in images in panels (a–f) and other time-points.

1900669 (3 of 7)
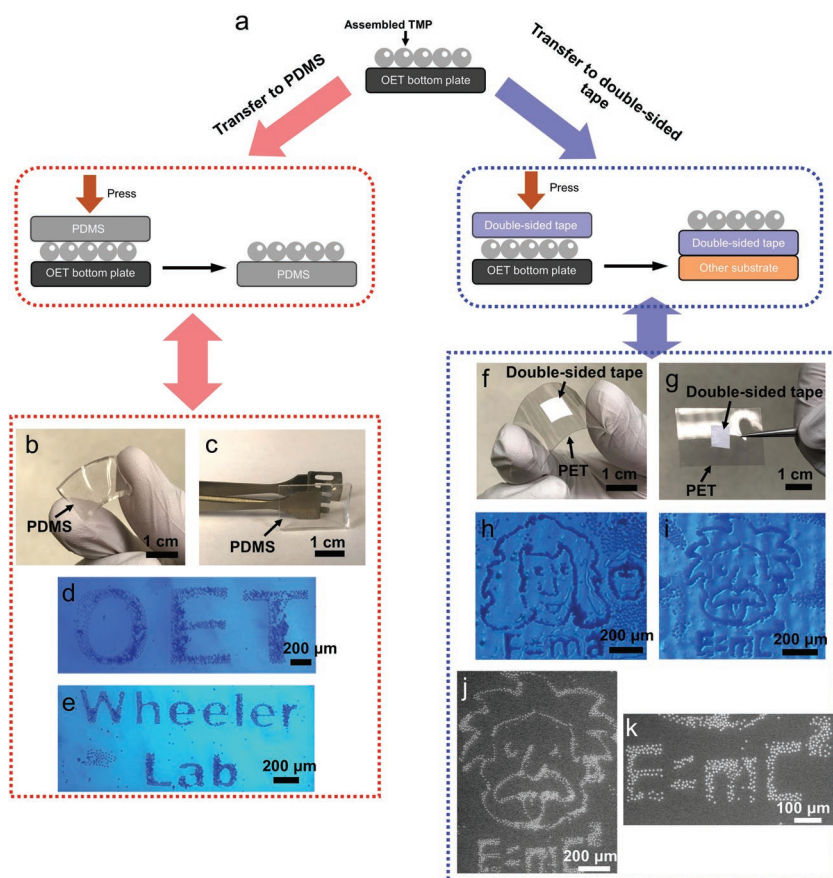
**Figure 4.** TMP transfer to destination substrates. a) Schematic illustration of the transfer of freeze-dried polystyrene-bead TMPs to PDMS (gray, in red-dashed box), and double-sided tape (blue, in blue-dashed box) substrates. The latter (double-sided tape) is then mounted on another substrate (orange). b,c) Images of PDMS substrate bearing transferred TMPs. d,e) Microscope images of the TMPs reading "OET" and "Wheeler Lab" after transfer to a PDMS substrate. f,g) Images of double-sided tape substrates (mounted on a PET backing) bearing transferred TMPs. h,i) Microscope images of TMPs depicting an Isaac Newton caricature with apple and Newton's second law of motion and an Albert Einstein caricature with the mass energy equation after transfer to a double-sided tape substrate. j,k) Scanning microscopy (SEM) images of the TMP-on-double-sided tape shown in (i).

3, 7.5, 10.5, and 20.3 s after projecting a light pattern in the shape of an "O." As indicated, the number of microbeads in the central illuminated region (inside the dashed red circle) decreases (driven by negative DEP) as time passes. Therefore, the change of the microbead density in the illuminated region should be a useful indicator of the TMP-formation process. Figure 3g is a plot of the grayscale intensity of the illuminated region of the microscope image (i.e., the area inside the dashed red circle) as a function of time. As shown, the grayscale intensity increases exponentially and then saturates after ≈15 s. We applied this technique to a number of different TMPs, with similar results—pattern formation was rapid, completing within 30 s for all of them. In the future, similar techniques might be used to measure fidelity between replicates of the same pattern.

After demonstrating capability for (i) assembling TMPs in liquid and (ii) removing the liquid medium via freeze-drying, we (iii) investigated the feasibility of transferring TMPs to

other substrates. After some trial-and-error, a reproducible technique was developed, illustrated in **Figure 4**a. As shown, two destination-substrates proved to be suitable for transfer: polydimethylsiloxane (PDMS) and double-sided tape. Figure 4b,c shows images of a PDMS substrate with a transferred TMP; Figure 4d,e shows microscope images of TMPs reading "OET" and "Wheeler Lab" after transfer to PDMS substrates. Figure 4f,g shows images of a double-sided tape substrate [adhered to a polyethylene terephthalate (PET) backing] with a transferred TMP; Figure 4h,i shows microscope images of Isaac Newton and Albert Einstein caricature-TMPs after transfer to double-sided tape substrates. Scanning electron microscope (SEM) images of the latter are also presented in Figure 4j,k, and SEM images of other assembled micropatterns on various substrates are shown in Figure S2 (Supporting Information).

During the transfer process, the PDMS substrate functions as an elastomeric stamp[42,43] which attracts the particles by kinetic adhesion; likewise, the chemical adhesive on the double-sided tape allows for collection of TMPs. The transferred TMPs described here are robust such that they withstand touching and bending (Figure 4b,f); quantitative analysis of the mechanical properties of transferred TMPs (which likely varies with initial particle-suspension density as well as particle–particle and particle–substrate adhesion) is an interesting topic for future study. An image comparison algorithm based on perceptual hashing[44] was developed to evaluate the fidelity of transfer for TMPs (the details of the algorithm and MATLAB code can be found in the Supporting Infor-

mation). As illustrated in Figure S3 (Supporting Information), the transfer-fidelity for a wide range of different TMPs (formed from different materials) transferred to PDMS or double-sided tape substrates was found to be high, with similarity indexes of all images evaluated found to be greater than 90%.

To evaluate the generality of the new technique, we explored patterning and transferring metallic particles and graphene nanoplatelets. These materials (in the conditions used here) have CM factors with opposite sign to that of polystyrene particles, and thus they experience a positive DEP force; as a result, "positive" images of the intended TMPs were used for these particles. **Figure 5**a–c shows the assembly of $Sn_{96.5}Ag_3Cu_{0.5}$ metal alloy beads into a "star" shaped TMP, the same TMP after freeze-drying, and the same TMP after transfer to a PDMS substrate. Figure 5d–f shows the assembly of graphene nanoplatelets into a "maple leaf" TMP, the same TMP after freeze-drying, and the same TMP after transfer to a PDMS
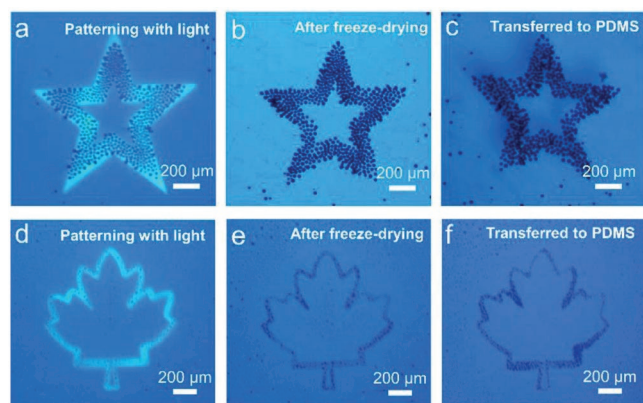
**Figure 5.** Assembly and transfer of metallic and graphene TMPs. Bright-field microscope images showing a) the illumination of a suspension of 15–25 µm diameter metallic particles with a light pattern depicting a positive "star" image, b) the resulting TMP after freeze-drying, and c) the resulting TMP after transfer to a PDMS substrate. Bright-field microscope images showing d) the illumination of a suspension of graphene nanoplatelets with a light pattern depicting a positive "maple leaf" image, e) the resulting TMP after freeze-drying, and f) the resulting TMP after transfer to a PDMS substrate.

substrate. These results are further evidence that the OET assembly, freeze-drying, and transfer method reported in this work is a general one that is widely applicable for different materials.

We propose that TMPs described here may eventually be useful to serve as security/identification markers of authenticity. As proof-of-concept, fluorescently labeled particles were used to form TMPs (which could potentially be "read" in terms of color, shape, and/or topography), which were then transferred to a range of objects. **Figure 6**a shows a photo of a Canadian $20 bill modified with a TMP formed from red fluorescent polystyrene beads; Figure 6b shows bright-field and fluorescent microscope images of the

transferred TMP. Figure 6c shows a photo of a nylon ribbon modified with a TMP formed from red fluorescent polystyrene beads; Figure 6d shows bright-field and fluorescent microscope images of the transferred TMP on the ribbon, which depicts "U of T" (the abbreviation for University of Toronto). Figure 6e shows a photo of a coin modified with a TMP formed from green fluorescent polystyrene beads; Figure 6f shows bright-field and fluorescent microscope images of the transferred TMP. Finally, Figure 6g shows the photoluminescence (PL) spectra of TMPs formed from green or red polystyrene beads, as measured using a 405 nm violet optical source and a spectrometer. All of the proof-of-principle applications described here rely on reversible modification of secondary substrates. But in the future, we propose that permanent modification strategies would be trivial to implement, with the potential to serve as anti-counterfeiting markers for official documentation, novelty micrologos for conferences or exhibitions, or (in combination with educational materials related to DEP and OET and Movie S1, Supporting Information) as activities and support for classroom/laboratory instruction.[45]

## 3. Conclusions

We have developed an optofluidic method for manufacturing TMPs. The method relies on OET to form patterns with arbitrary shape and form, combined with an innovative freeze-drying and transfer process to apply the TMPs to different substrates. We characterized the negative and positive DEP forces used to form the TMPs, and demonstrated good fidelity between design and finished product. We propose that TMPs formed in this manner have the potential to serve anti-counterfeiting markers for official documentation, novelty micrologos for scientific conferences and exhibitions, or to support classroom/laboratory instruction.
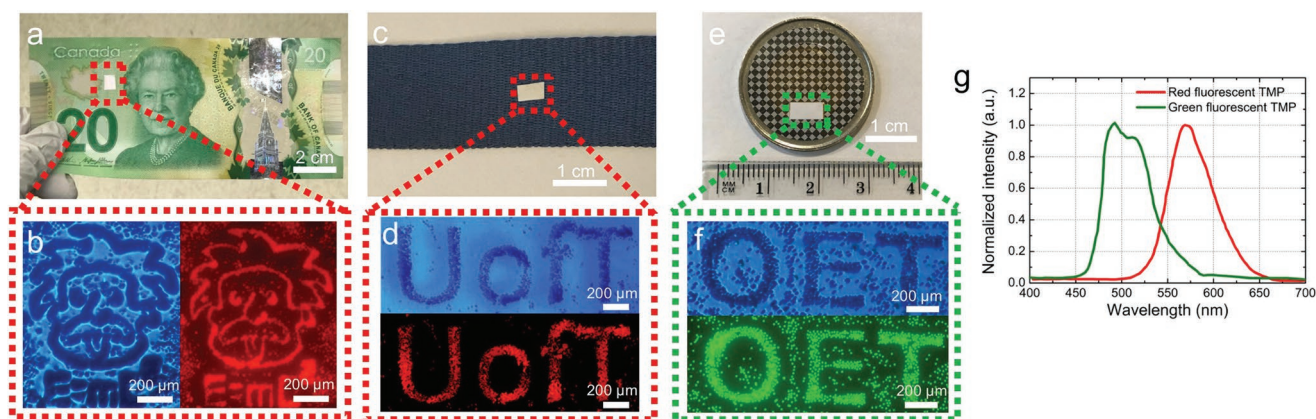


**Figure 6.** Proof-of-concept applications for OET-TMPs. a) Image of a Canadian $20 bill modified with a red-fluorescent TMP, included with permission from the Bank of Canada (noting that the Bank of Canada was not involved in this research). b) Bright-field (left) and fluorescence microscopy (right) images of an Albert Einstein caricature TMP on a $20 bill. c) Image of a fabric ribbon modified with a red-fluorescent TMP. d) Bright-field (top) and fluorescence microscopy (bottom) images of a TMP that depict "U of T" (the abbreviation for the University of Toronto) on a nylon fabric ribbon. e) Image of a coin modified with a green-fluorescent TMP. f) Bright-field (top) and fluorescence microscopy (bottom) images of a TMP that depict "OET" on a coin. g) PL spectra of assembled red and green fluorescent TMPs.

ADVANCED
SCIENCE NEWS
www.advancedsciencenews.com

ADVANCED
OPTICAL
MATERIALS
www.advopticalmat.de

## 4. Experimental Section

*Instrumentation and OET*: Detailed descriptions of the OET instrument (featuring a projector interfaced to a microscope) and OET devices can be found in previous reports.[40,41] When completed, devices comprised a 20 µL chamber sandwiched between a top and bottom plate (each plate bearing a 200-nm-thick ITO electrode), with the bottom plate featuring a 1 µm thick layer of a-Si:H deposited by radio frequency plasma enhanced chemical vapor deposition (RF-PECVD). A custom microscope-stage insert was developed featuring a Peltier cooler (Mouser Electronic, CP50441) and a 3D-printed tray to contain dry ice. Unless otherwise specified, OET devices were driven at an AC applied bias of 20 $V_{p-p}$ at 20 kHz.

*Preparation of Samples for OET Manipulation*: Three kinds of polystyrene microspheres (with nominal average diameters provided by the supplier, Polysciences) were used in this work: 6-µm-diameter microbeads with red fluorescent markers, 10-µm-diameter microbeads with green fluorescent markers, and 10-µm-diameter microbeads with no fluorescent markers. The metallic beads used in this work are $Sn_{96.5}Ag_3Cu_{0.5}$ microspheres with diameters ranging from 15 to 25 µm (Industrie des Poudres Sphériques). The graphene particles used in this work are graphene nanoplatelets (Sigma-Aldrich, 799084) which are in powder form as provided by the supplier. Prior to experiments particles were suspended at 0.1 to $1 \times 10^7$ particles $mL^{-1}$ in deionized (DI) water containing 0.05% (v/v) Tween 20 (P9416 SIGMA), which has a conductivity of 5.0 mS $m^{-1}$. In typical experiments, a 20 µL aliquot of the suspension (polystyrene beads, metallic beads, or graphene nanoplatelets) was pipetted into the chamber of the OET device, which was then positioned on the microscope where the microassembly process was performed.

*TMP Formation and Freeze-Drying*: In a typical experiment, a suspension of particles in aqueous medium was organized into a pattern using OET. Upon formation (with OET biased and light pattern still illuminating the sample), dry ice was inserted into the custom tray, and the Peltier cooler was driven with DC current (2 A) until the liquid medium was visibly frozen (≈2 min). The OET device was then removed from the microscope and incubated at −80 °C in a freezer (Thermal Scientific Forma 900) for 5 min. The device was then inserted into a freeze-dryer (LABCONCO, 7752020) for 30 min to sublimate the frozen medium.

*TMP Transfer and Characterization*: After freeze-drying, TMPs were transferred to PDMS (Sylgard 184) or double-sided tape (3M 9965 medical tape) substrates. PDMS substrates were formed by mixing a curing agent to prepolymer (1:10 wt/wt), loading into a 15 cm diameter Petri dish and curing at 80 °C for 1 h. The resulting PDMS film (≈3 mm thick) was peeled off and sectioned into small pieces before use. In a typical TMP transfer, the designated substrate was positioned gently on top of an OET bottom plate bearing a freeze-dried TMP. Then, a hand-held mini roller was used to roll over the assembly to ensure even contact. Finally, the substrate was gently peeled away from the OET bottom plate for OET-transfer characterization. Double-sided tape was useful for transfer of TPMs to other substrates including PET pieces (Sigma-Aldrich 639303, 0.13 mm thickness), a Canadian $20 bill, a nylon ribbon with University of Toronto logo, or a Canadian $2 coin. Note that the tape is opaque, such that it appears as a white rectangle in photographs. TMPs were characterized by bright-field microscopy or scanning electron microscope (see the Supporting Information). Some fluorescent TMPs were characterized by fluorescence microscopy, and/or by photoluminescence spectroscopy using a 405 nm violet source (Laserglow Technologies, LRD-0405) coupled to a mini-spectrometer (OceanOptics QEPro).

## Supporting Information

Supporting Information is available from the Wiley Online Library or from the author.

## Conflict of Interest

The authors declare no conflict of interest.

[1] B. Ellis, M. A. Mayer, G. Shambat, T. Sarmiento, J. Harris, E. E. Haller, J. Vučković, *Nat. Photonics* **2011**, *5*, 297.

[2] Q. Lin, B. Hua, S. F. Leung, X. Duan, Z. Fan, *ACS Nano* **2013**, *7*, 2725.

[3] J. D. Caldwell, O. Glembocki, F. J. Bezares, N. D. Bassim, R. W. Rendell, M. Feygelson, M. Ukaegbu, R. Kasica, L. Shirey, C. Hosten, *ACS Nano* **2011**, *5*, 4046.

[4] F. De Angelis, F. Gentile, F. Mecarini, G. Das, M. Moretti, P. Candeloro, M. L. Coluccio, G. Cojoc, A. Accardo, C. Liberale, R. P. Zaccaria, G. Perozziello, L. Tirinato, A. Toma, G. Cuda, R. Cingolani, E. D. Fabrizio, *Nat. Photonics* **2011**, *5*, 682.

[5] L. R. Huang, E. C. Cox, R. H. Austin, J. C. Sturm, *Science* **2004**, *304*, 987.

[6] Z. Wang, H. J. Wu, D. Fine, J. Schmulen, Y. Hu, B. Godin, J. X. Zhang, X. Liu, *Lab Chip* **2013**, *13*, 2879.

[7] B. Dura, S. K. Dougan, M. Barisa, M. M. Hoehl, C. T. Lo, H. L. Ploegh, J. Voldman, *Nat. Commun.* **2015**, *6*, 5940.

[8] W. Zhu, J. Li, Y. J. Leong, I. Rozen, X. Qu, R. Dong, Z. Wu, W. Gao, P. H. Chung, J. Wang, S. Chen, *Adv. Mater.* **2015**, *27*, 4411.

[9] B. C. Gross, J. L. Erkal, S. Y. Lockwood, C. Chen, D. M. Spence, *Anal. Chem.* **2014**, *86*, 3240.

[10] F. Kotz, K. Arnold, W. Bauer, D. Schild, N. Keller, K. Sachsenheimer, T. M. Nargang, C. Richter, D. Helmer, B. E. Rapp, *Nature* **2017**, *544*, 337.

[11] A. K. Dubey, V. Yadava, *Int. J. Mach. Tools Manuf.* **2008**, *48*, 609.

[12] A. Carlson, A. M. Bowen, Y. Huang, R. G. Nuzzo, J. A. Rogers, *Adv. Mater.* **2012**, *24*, 5284.

[13] T. H. Kim, K. S. Cho, E. K. Lee, S. J. Lee, J. Chae, J. W. Kim, D. H. Kim, J. Y. Kwon, G. Amaratunga, S. Y. Lee, B. L. Choi, Y. Kuk, J. M. Kim, K. Kim, *Nat. Photonics* **2011**, *5*, 176.

**ADVANCED
SCIENCE NEWS**

www.advancedsciencenews.com

**ADVANCED
OPTICAL
MATERIALS**

www.advopticalmat.de

[14] S. Y. Tang, J. Zhu, V. Sivan, B. Gol, R. Soffe, W. Zhang, A. Mitchell, K. Khoshmanesh, *Adv. Funct. Mater.* **2015**, *25*, 4445.

[15] R. J. Barsotti, M. D. Vahey, R. Wartena, M. Chiang, J. Voldman, F. Stellacci, *Small* **2007**, *3*, 488.

[16] R. Pethig, *Biomicrofluidics* **2010**, *4*, 022811.

[17] X. Ding, S. C. S. Lin, B. Kiraly, H. Yue, S. Li, I. K. Chiang, J. Shi, S. J. Benkovic, T. J. Huang, *Proc. Natl. Acad. Sci. USA* **2012**, *109*, 11105.

[18] J. P. Lata, F. Guo, J. Guo, P. H. Huang, J. Yang, T. J. Huang, *Adv. Mater.* **2016**, *28*, 8632.

[19] S. Orbay, A. Ozcelik, H. Bachman, T. J. Huang, *J. Micromech. Microeng.* **2018**, *28*, 025012.

[20] A. Snezhko, I. S. Aranson, *Nat. Mater.* **2011**, *10*, 698.

[21] I. D. Vlaminck, C. Dekker, *Annu. Rev. Biophys.* **2012**, *41*, 453.

[22] D. G. Grier, *Nature* **2003**, *424*, 810.

[23] M. Woerdemann, S. Gläsener, F. Hörner, A. Devaux, L. De Cola, C. Denz, *Adv. Mater.* **2010**, *22*, 4176.

[24] G. R. Kirkham, E. Britchford, T. Upton, J. Ware, G. M. Gibson, Y. Devaud, M. Ehrbar, M. Padgett, S. Allen, L. D. Buttery, K. Shakesheff, *Sci. Rep.* **2015**, *5*, 8577.

[25] O. M. Maragò, P. H. Jones, P. G. Gucciardi, G. Volpe, A. C. Ferrari, *Nat. Nanotechnol.* **2013**, *8*, 807.

[26] P. Y. Chiou, A. T. Ohta, M. C. Wu, *Nature* **2005**, *436*, 370.

[27] M. C. Wu, *Nat. Photonics* **2011**, *5*, 322.

[28] A. Jamshidi, P. J. Pauzauskie, P. J. Schuck, A. T. Ohta, P. Y. Chiou, J. Chou, P. Yang, M. C. Wu, *Nat. Photonics* **2008**, *2*, 86.

[29] A. Jamshidi, S. L. Neale, K. Yu, P. J. Pauzauskie, P. J. Schuck, J. K. Valley, H. Y. Hsu, A. T. Ohta, M. C. Wu, *Nano Lett.* **2009**, *9*, 2921.

[30] M. Woerdemann, C. Alpmann, M. Esseling, C. Denz, *Laser Photonics Rev.* **2013**, *7*, 839.

[31] S. Zhang, Y. Liu, J. Juvert, P. Tian, J. C. Navarro, J. M. Cooper, S. L. Neale, *Appl. Phys. Lett.* **2016**, *109*, 221110.

[32] M. B. Lim, R. G. Felsted, X. Zhou, B. E. Smith, P. J. Pauzauskie, *Appl. Phys. Lett.* **2018**, *113*, 031106.

[33] S. M. Yang, T. M. Yu, H. P. Huang, M. Y. Ku, L. Hsu, C. H. Liu, *Opt. Lett.* **2010**, *35*, 1959.

[34] I. Elvira, J. F. Muñoz-Martínez, Á. Barroso, C. Denz, J. B. Ramiro, A. García-Cabañes, F. Agulló-López, M. Carrascosa, *Opt. Lett.* **2018**, *43*, 30.

[35] S. Zhang, A. Nikitina, Y. Chen, Y. Zhang, L. Liu, A. G. Flood, J. Juvert, M. D. Chamberlain, N. P. Kherani, S. L. Neale, A. R. Wheeler, *Opt. Express* **2018**, *26*, 5300.

[36] L. Y. Ke, Z. K. Kuo, Y. S. Chen, T. Y. Yeh, M. Dong, H. W. Tseng, C. H. Liu, *Lab Chip* **2018**, *18*, 106.

[37] H. Hwang, J. K. Park, *Lab Chip* **2011**, *11*, 33.

[38] S. Zhang, J. Juvert, J. M. Cooper, S. L. Neale, *Sci. Rep.* **2016**, *6*, 32840.

[39] S. L. Neale, M. Mazilu, J. I. B. Wilson, K. Dholakia, T. F. Krauss, *Opt. Express* **2007**, *15*, 12619.

[40] S. Zhang, N. Shakiba, Y. Chen, Y. Zhang, P. Tian, J. Singh, M. D. Chamberlain, M. Satkauskas, A. G. Flood, N. P. Kherani, S. Yu, P. W. Zandstra, A. R. Wheeler, *Small* **2018**, *14*, 1803342.

[41] S. Zhang, Y. Liu, Y. Qian, W. Li, J. Juvert, P. Tian, J. C. Navarro, A. W. Clark, E. Gu, M. D. Dawson, J. M. Cooper, S. L. Neale, *Opt. Express* **2017**, *25*, 28838.

[42] M. A. Meitl, Z.-T. Zhu, V. Kumar, K. J. Lee, X. Feng, Y. Y. Huang, I. Adesida, R. G. Nuzzo, J. A. Rogers, *Nat. Mater.* **2006**, *5*, 33.

[43] A. J. Trindade, B. Guilhabert, D. Massoubre, D. Zhu, N. Laurand, E. Gu, I. M. Watson, C. J. Humphreys, M. D. Dawson, *Appl. Phys. Lett.* **2013**, *103*, 253302.

[44] X. M. Niu, Y. H. Jiao, *Acta Electron. Sin.* **2008**, *36*, 1405.

[45] P. Y. Chiou, Interactive microparticle manipulation using OET [Video file], https://www.youtube.com/watch?v=_FkROvhVzCo&list=UUX6e2chk7w6xSDQLcdG1UKQ&index=19 (accessed: September 2019).